J. Indian Chem. Soc.,
Vol. 96, February 2019, pp. 269-274

Synthesis and hydrogen storage performance of Al_2O_3 nanoparticle decorated functionalized multi-walled carbon nanotubes (Al_2O_3@f-MWCNTs)

Madhavi Konni and Saratchandra Babu Mukkamala*

Nanoscience & Nanotechnology Laboratory, Department of Chemistry, Institute of Science, GITAM (Deemed University), Visakhapatnam-530 045, Andhra Pradesh, India

E-mail: mscbabu@gmail.com

Manuscript received online 02 December 2018, revised 30 January 2019, accepted 31 January 2019

Al_2O_3 nanoparticle decorated functionalized Multi-Walled Carbon Nanotubes (Al_2O_3@f-MWCNTs) have been synthesized to examine the hydrogen storage performance at non-cryogenic temperatures and moderate pressures for green energy applications. The experimental conditions such as solvent medium and metal content have been tuned to improve the decoration of Al_2O_3 nanoparticles on the surface of carboxylate-functionalized multi-walled carbon nanotubes (COOH-MWCNTs/f-MWCNTs). The morphology, surface properties and structure of compounds were characterized by Scanning Electron Microscopy (SEM), Transmission Electron Microscopy (TEM), FT-IR and powder X-ray diffraction. The hydrogen uptake of materials was examined by High Pressure Gas Adsorption System at non-cryogenic temperatures i.e. 253 K and 298 K up to 70 bar pressure. Al_2O_3@f-MWCNTs prepared in water, triethylamine and DMF adsorbed 0.46, 0.55 and 0.67 wt% of hydrogen at 253 K and 0.17, 0.31 and 0.46 wt% of hydrogen at 298 K, respectively. The higher uptake of hydrogen by Al_2O_3@f-MWCNTs prepared in DMF is due to uniform loading of metal nanoparticles on the surface of carbon nanotubes.

Keywords: Functionalization, P-MWCNTs, f-MWCNTs, Al_2O_3 nanoparticles, hydrogen storage.

Introduction

Hydrogen is considered as a future fuel due to its high energy content (143 MJ/Kg) and eco-friendly characteristics. Storage of hydrogen is a key enabling technology for onboard vehicle applications. Physical techniques such as high pressure and cryogenic storage methods are not ideal for transport applications, due to the risk associated with them[1–3]. Extensive research has been focused on the development of solid-state storage medium for hydrogen over the last few decades but none of them matched with the targets set by U.S. Department of Energy (DOE) (7.5 wt% at non-cryogenic conditions)[4–6]. Carbon-based materials such as graphene, carbon nanotubes and C_{60} are considered to be promising a hydrogen storage medium because of their lightweight, pore structure and high surface area[7–12]. However, at room temperature, due to weak van der Waals interaction and low binding energy (0.11 eV), pristine carbon nanostructures exhibit poor hydrogen uptake[13–15]. But the binding energy of 0.20–0.60 eV is necessary for sufficient hydrogen uptake to meet the DOE target for onboard transport applications[16–18]. Hydrogen uptake capacity can be enhanced by increasing the binding energy of carbon nanostructures through decorating with alkali (Li, Na and K)[19,20], alkaline earth (Be, Mg and Ca)[7,21–23], transition metals (Sc, Ti, V, Pd and Pt)[24–26], and metal hydrides[27–29].

Alumina (Al_2O_3) is thermodynamically stable crystalline material and commonly using as ceramic composite[30], cements and liners[31], synthetic biomaterial[32]. Recent reports show that Al-modified graphene is recommended for hydrogen storage as well as gas sensor applications. Ao *et al.*[33,34] reported that Al-doped graphene can store H_2 molecules up to 5.13 wt% at 300 K and 0.1 GPa. The adsorption binding energy observed in this case is 0.260 eV/H_2. Further, as reported by Ao and Peeters[35], Al loaded graphene could adsorb 13.79 wt% of hydrogen at an average binding energy of 0.193 eV/H_2 calculated through DFT. Carrete *et al*. predicted through DFT calculations that Al decorated graphene nanoribbons (GNRs) can adsorb a sufficient amount of hydrogen to meet the DOE targets. Another recent theoretical study shows that Al-decorated porous graphene adsorbs 10.5 wt% of hydrogen with an enhanced binding energy of 0.41 eV/H_2[36]. So, to the best of our knowledge, there are very

few reports on the experimental investigation of hydrogen storage behaviour of Al_2O_3/MWCNTs nanoparticles. In this paper, the influence of different solvents such as water, amine and DMF on the decoration of nanoparticles on surface f-MWCNTs and hydrogen storage performance at non-cryogenic temperatures and moderate pressures are presented.

Experimental

Materials:

$Al(NO_3)_3.9H_2O$ and triethylamine purchased from Merck, India and dimethylformamide (DMF) was procured from Fisher Scientific.

Functionalization of MWCNTs:

0.3 g of purified multi-walled carbon nanotubes (p-MWCNTs) and 150 ml nitration mixture (1:3 HNO_3 and H_2SO_4) were refluxed for 48 h under magnetic stirring. The obtained functionalized MWCNTs (COOH-MWCNTs/f-MWCNTs) were washed with the deionized water and dried overnight in vacuum at 40°C.

Preparation of Al_2O_3@f-MWCNTs:

200 mg of carboxylate functionalized MWCNTs (f-MWCNTs) and 7.50 g [0.02 mol, High metal concentration (HMC)] or 3.75 g [0.01 mol, Low metal concentrations (LMC)] of $Al(NO_3)_3$ were taken in a 500 ml round bottomed flask. To this, 150 ml distilled water/150 ml distilled water containing 0.5 ml triethylamine (TEA)/150 ml dimethylformamide (DMF) was mixed thoroughly and heated at 80°C for 6 h (solution pH of the aqueous medium was ~7.0 and TEA medium was ~10.0). The resulting solid was washed till the pH of washing was neutral. The sample was dried overnight in vacuum at 40°C.

Characterization methods:

FEI Quanta 200 FEG Scanning Electron Microscope (SEM) and Philips CM 200 Transmission Electron Microscope (TEM) are used to examine the morphology/texture of synthesized compounds. The FT-IR spectra of samples were measured using Perkin-Elmer Spectrum two spectrophotometer. Diffraction patterns were recorded with the help of PANalytical X'Pert PRO powder X-ray diffractometer with graphite monochromatic CuKα (λ = 1.5406 Å) radiation. The BET surface area was determined using Quantachrome NOVA 1200e. High-pressure gas adsorption system (BELSORP-HP) is used for hydrogen gas sorption measurements.

Results and discussion

The surface morphology of Al_2O_3 nanoparticle decorated MWCNTs was examined by Scanning Electron Microscopy (SEM) and Transmission Electron Microscopy (TEM). Fig. 1 shows the SEM image of Al_2O_3@f-MWCNTs. The surface of MWCNTs displays that carbon nanotube measures about 20–40 nm diameter with few micrometres length. The presence

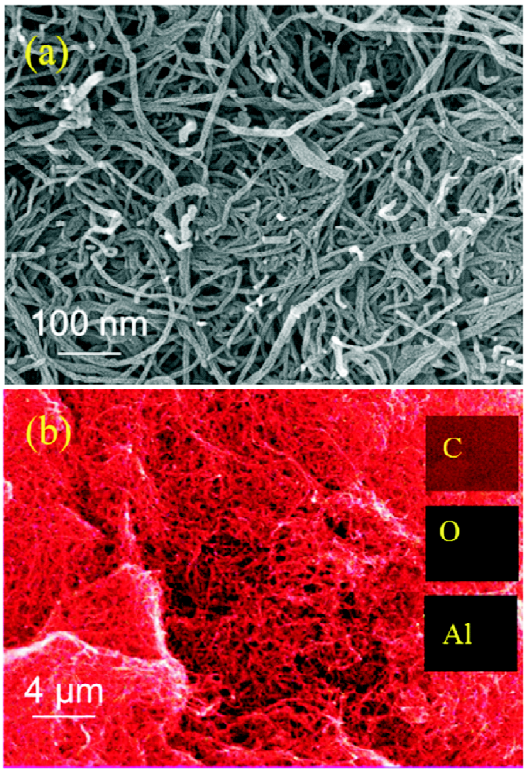

Fig. 1. (a) SEM image of Al_2O_3@f-MWCNTs and (b) SEM image of Al_2O_3@f-MWCNTs with elemental mapping.

of MWCNTs along with Al_2O_3 nanoparticles is confirmed from this SEM image together with the corresponding elemental mapping. The EDAX measurements (Fig. 2) show the composition of carbon, oxygen, aluminium from Al_2O_3@f-MWCNTs. The TEM images (Fig. 3) reveals that Al_2O_3 nanoparticles were successfully loaded on the surface of CNTs. It was seen from the TEM images (Fig. 3a) that in Al_2O_3@f-MWCNTs, the spherical alumina (Al_2O_3) nanoparticles were found to be uniformly distributed covering a large area of the nanotube network. The size of the metal oxide nanoparticles varied from 5 to 20 nm.

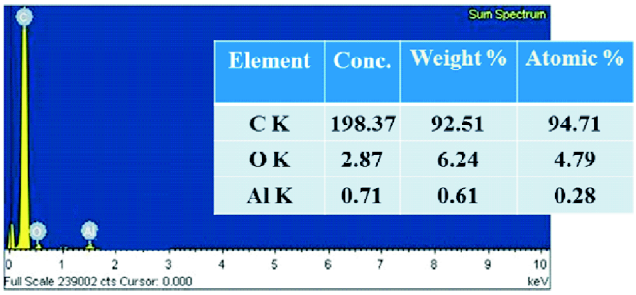

Fig. 2. EDAX image of Al_2O_3@f-MWCNTs.

tion of pores of the p-MWCNTs by COOH functional groups after surface functionalization. The surface area is further reduced from 236 m^2/g to 206, 194 and 23 m^2/g for Al_2O_3@f-MWCNTs prepared in water, amine and DMF, respectively. This decrease in surface area is due to blocking of some more pores by Al_2O_3 nanoparticles.

The hydrogen adsorption capacities of Al_2O_3 decorated MWCNTs along with pristine and functionalized MWCNTs were measured volumetrically at 253 K and 298 K at moderate pressures i.e. up to 70 bar using high-pressure gas sorption analyser, BELSORP-HP. Adsorption of hydrogen on MWCNTs and Al_2O_3@f-MWCNTs is reversible (Fig. 6), so desorption curves are omitted in all hydrogen uptake illustrations for clarity. It was observed that the hydrogen adsorption capacity of pristine and f-MWCNTs at 253 K and 70

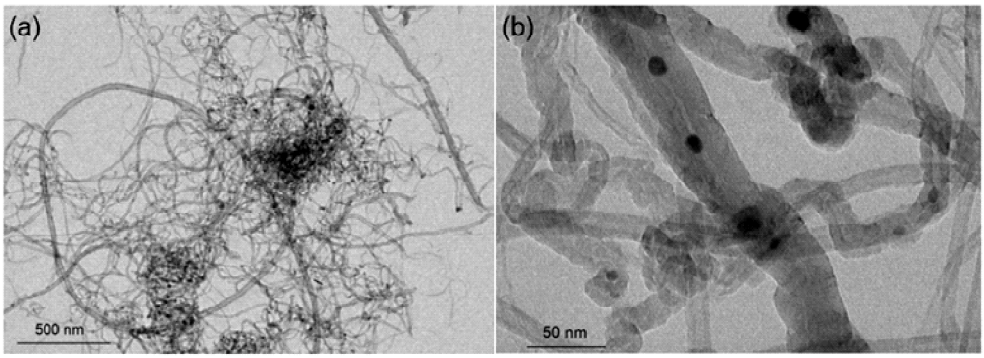

Fig. 3. (a) TEM image of Al_2O_3@f-MWCNTs and (b) magnified TEM image of Al_2O_3@f-MWCNTs.

The FT-IR spectra of pristine-MWCNTs, f-MWCNTs, and Al_2O_3@f-MWCNTs are shown in Fig. 4. The two peaks at 2920 cm^{-1} and 2854 cm^{-1} corresponding to the C-H stretching vibrations. The adsorption peak at 1682 cm^{-1} corresponding to the stretching vibration of C=O from -COOH. This indicates the formation of functionalized MWCNTs (COOH-MWCNTs/f-MWCNTs) (Fig. 4a and 4b). The peak at 655 cm^{-1} corresponds to the Al-O bond.

Fig. 5 shows the powder X-ray diffraction patterns of the pristine MWCNTs and Al_2O_3@f-MWCNTs. The diffraction pattern shows broad 2 theta peaks around 25.4° and 42.9° corresponding to the (101) and (100) reflections of CNTs, respectively. The diffraction peaks (Fig. 5b) at 19.2°, 20.1°, 37.4° and 39.9° correspond to (111), (012), (110) and (113) planes of Al_2O_3 nanoparticles, respectively.

The BET specific surface area of p-MWCNTs, f-MWCNTs and Al_2O_3@f-MWCNTs determined by N_2 absorption measurements at 77 K are shown in Table 1. The surface area of p-MWCNTs and f-MWCNTs is 360 m^2/g and 236 m^2/g, respectively. This decrease in surface area is due to occupa-

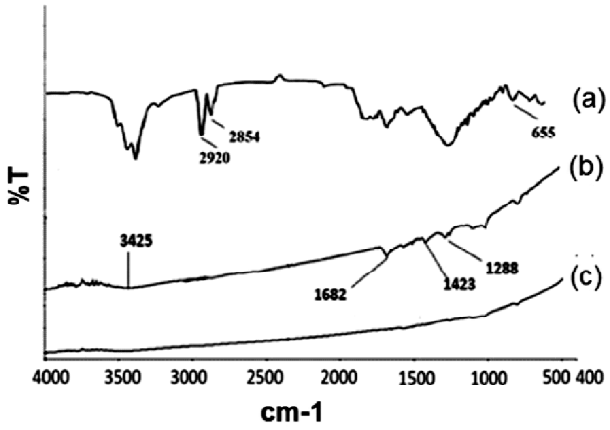

Fig. 4. FT-IR spectra of (a) Al_2O_3@f-MWCNTs, (b) f-MWCNTs and (c) p-MWCNTs.

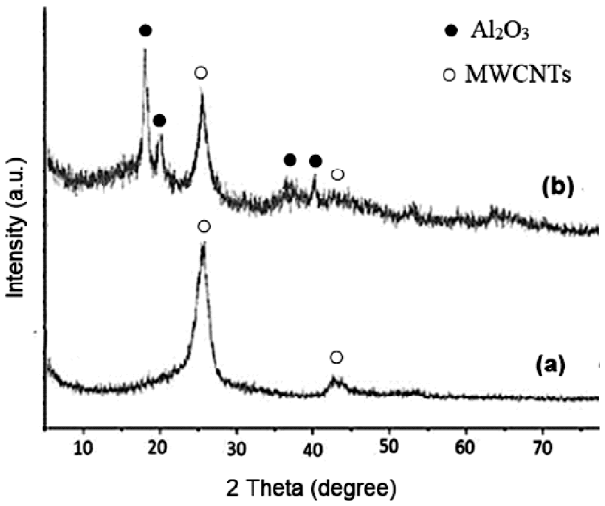

Fig. 5. Powder XRD patterns of (a) p-MWCNTs and (b) Al_2O_3@f-MWCNTs.

Table 1. BET surface area and hydrogen uptake capacity of Al_2O_3@f-MWCNTs

Sample	Reaction medium	^{s}BET (m^2/g)	H_2 uptake at 253 K and 70 bar (wt%)	H_2 uptake at 298 K and 70 bar (wt%)
p-MWCNTs	–	360	0.30	0.12
f-MWCNTs	–	236	0.09	0.06
Al_2O_3@f-MWCNTs	Water	206	0.31[a]	0.13[a]
			0.46[b]	0.17[b]
Al_2O_3@f-MWCNTs	Triethyl-amine	194	0.42[a]	0.22[a]
			0.55[b]	0.31[b]
Al_2O_3@f-MWCNTs	DMF	23	0.46[a]	0.31[a]
			0.67[b]	0.46[b]

[a]LMC – Low metal concentration. [b]HMC – High metal concentration.

bar pressure was 0.31 and 0.09 wt%, respectively. At 298 K the hydrogen adsorption capacity of pristine and COOH-MWCNTs was 0.12 and 0.06 wt%, respectively. So, it was observed that at low temperatures material exhibited high uptake capacity compared to room temperatures. Al_2O_3@f-MWCNTs prepared at LMC in water, triethylamine and DMF adsorb 0.31, 0.42 and 0.46 wt% of hydrogen (Fig. 7) whereas Al_2O_3@f-MWCNTs prepared at HMC adsorbs 0.46, 0.55 and 0.67 wt% (Fig. 8), respectively at 253 K. This result indicates that the hydrogen sorption property drastically increases on increasing the Al_2O_3 nanoparticle content on surface of f-MWCNTs. Fig. 9 shows that the hydrogen adsorption iso-

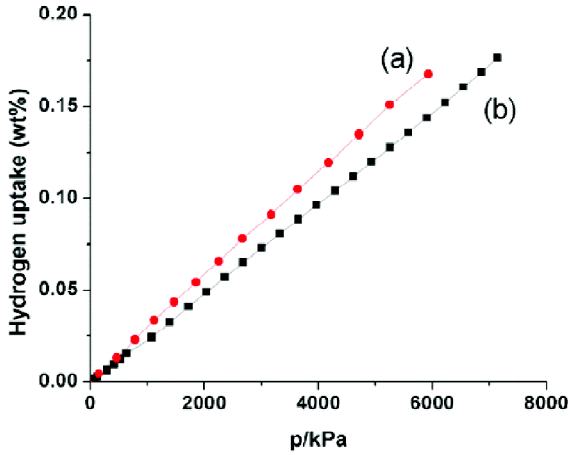

Fig. 6. Hydrogen sorption by Al_2O_3@f-MWCNTs in TEA at 298 K at HMC: (a) desorption and (b) adsorption.

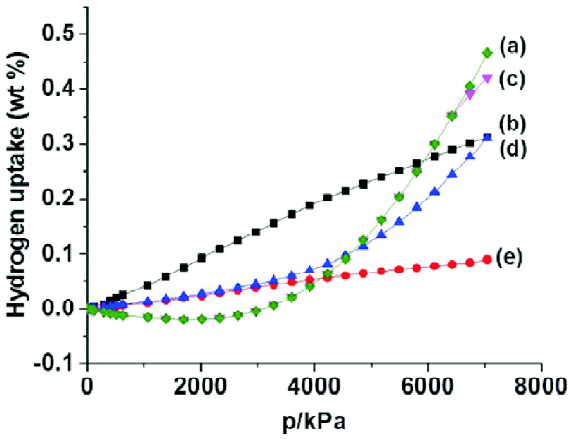

Fig. 7. Hydrogen storage by MWCNTs at 253 K at LMC: (a) Al_2O_3@f-MWCNTs in DMF, (b) p-MWCNTs, (c) Al_2O_3@f-MWCNTs in TEA, (d) Al_2O_3@f-MWCNTs in H_2O and (e) COOH-MWCNTs.

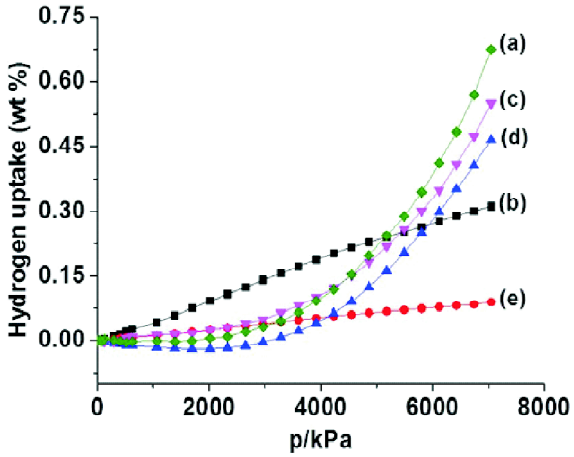

Fig. 8. Hydrogen storage by MWCNTs at 253 K at HMC: (a) Al_2O_3@f-MWCNTs in DMF, (b) p-MWCNTs, (c) Al_2O_3@f-MWCNTs in TEA, (d) Al_2O_3@f-MWCNTs in H_2O and (e) COOH-MWCNTs.

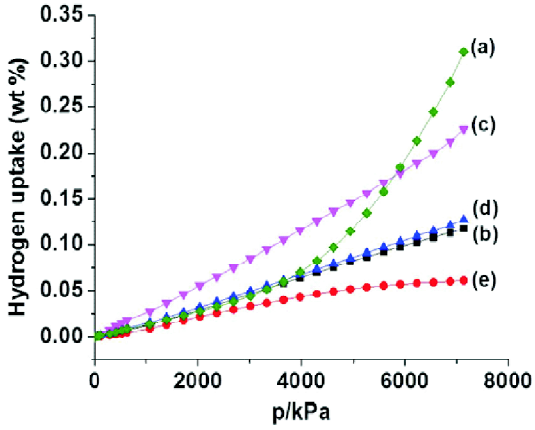

Fig. 9. Hydrogen storage by MWCNTs at 298 K at LMC: (a) Al_2O_3@f-MWCNTs in DMF, (b) p-MWCNTs, (c) Al_2O_3@f-MWCNTs in TEA, (d) Al_2O_3@f-MWCNTs in H_2O and (e) COOH-MWCNTs.

therms recorded at 298 K for Al_2O_3@f-MWCNTs prepared at LMC in water, triethylamine and DMF indicated 0.13, 0.22 and 0.31 wt% of adsorption. Similarly, Al_2O_3@f-MWCNTs prepared at HMC under the aforementioned reaction conditions adsorbed 0.17, 0.31 and 0.46 wt% of hydrogen (Fig. 10). The data on the hydrogen storage capacity of Al_2O_3@f-MWCNTs is presented in Table 1. The higher uptake observed by Al_2O_3@f-MWCNTs is due to spillover effect (dissociation of molecular hydrogen by Al_2O_3 and transported as atomic hydrogen to the surface of MWCNTs).

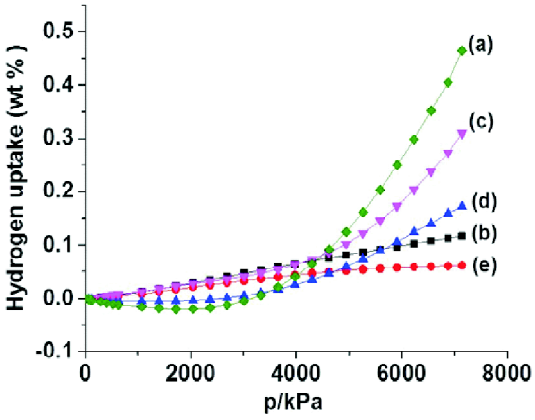

Fig. 10. Hydrogen storage by MWCNTs at 298 K at HMC: (a) Al_2O_3@f-MWCNTs in DMF, (b) p-MWCNTs, (c) Al_2O_3@f-MWCNTs in TEA, (d) Al_2O_3@f-MWCNTs in H_2O and (e) COOH-MWCNTs.

Conclusions

In this paper, the hydrogen storage performance of Al_2O_3 nanoparticle decorated f-MWCNTs examined at non-cryogenic conditions is presented. The hydrogen storage capacity of Al_2O_3@f-MWCNTs was 0.67 and 0.46 wt% at 253 and 298 K, respectively, which exhibited 2–3 times higher than the pristine-MWCNTs. Solvent and metal content play a key role in the decoration of Al_2O_3 on the surface of MWCNTs as well as on hydrogen storage performance.

Acknowledgements

This work was supported by the University Grants Commission (UGC), Govt. of India (Project No.: 42-258/2013 (SR)). The authors also acknowledge the SAIF, IIT, Bombay for assistance with TEM measurements.

References

1. Y. Demirel, "Energy: production, conversion, storage, conservation, and coupling", Springer-Verlag, London, 2012.
2. L. Schlapbach and A. Züttel, "Hydrogen-storage materials for mobile applications", in 'Materials for sustainable energy: a collection of peer-reviewed research and review articles from nature publishing group', 2011, 265.
3. R. F. Service, *Science*, 2004, **305**, 958.
4. C. C. Huang, N. W. Pu, C. A. Wang, J. C. Huang, Y. Sung and M. D. Ger, *Sep. Purif. Technol.*, 2011, **82**, 210.
5. H. P. Zhang, X. G. Luo, X. Y. Lin, X. Lu and Y. Leng, *Int. J. Hydrog. Energy*, 2013, **38**, 14269.
6. B. P. Vinayan, K. Sethupathi and S. Ramaprabhu, *Int. J. Hydrog. Energy*, 2013, **38**, 2240.
7. T. Hussain, B. Pathak, M. Ramzan, T. A. Maark, R. Ahuja and A. De Sarkar, *Appl. Phys. Lett.*, 2012, **100**, 183902.
8. A. Reyhani, S. Z. Mortazavi, S. Mirershadi, A. Z. Moshfegh, P. Parvin and A. N. Golikand, *J. Phys. Chem. C*, 2011, **115**, 6994.
9. D. G. Narehood, J. V Pearce, P. C. Eklund, P. E. Sokol, R. E. Lechner and J. Pieper, *Phys. Rev. B*, 2003, **67**, 205409.
10. A. C. Dillon, K. M. Jones, T. A. Bekkedahl, C. H. Kiang, D. S. Bethune and M. J. Heben, *Nature*, 1997, **386**, 377.
11. Z. M. Ao, Q. Jiang, R. Q. Zhang, T. T. Tan and S. Li, *J. Appl. Phys.*, 2009, **105**, 074307.
12. K. M. Fair, X. Y. Cui, L. Li, C. C. Shieh, R. K. Zheng and Z. W. Liu, *Phys. Rev. B*, 2013, **87**, 014102.
13. J. S. Arellano, L. M. Molina, A. Rubio, M. J. Lopez and J. A. Alonso, *J. Chem. Phys.*, 2002, **117**, 2281.
14. D. G. Narehood, J. V Pearce, P. C. Eklund, P. E. Sokol, R. E. Lechner and J. Pieper, *Phys. Rev. B*, 2003, **67**, 205409.
15. B. K. Pradhan, G. U. Sumanasekera, K. W. Adu, H. E. Romero, K. A. Williams and P. C. Eklund, *J. Phys. B*, 2002, **323**, 115.
16. S. K. Bhatia and A. L. Myers, *Langmuir*, 2006, **22**, 1688.

17. R. C. Lochan and M. Head-Gordon, *Phys. Chem. Chem. Phys*., 2006, **8**, 1357.
18. US Department of Energy, Targets for onboard hydrogen storage systems for light-duty vehicles, Office of Energy, 2009, 1.
19. W. Liu, Y. H. Zhao, Y. Li, Q. Jiang and E. J. Lavernia, *J. Phys. Chem. C*, 2009, **113**, 2028.
20. F. D. Wang, F. Wang, N. N. Zhang, Y. H. Li, S. W. Tang and H. Sun, *Chem. Phys. Lett.*, 2013, **555**, 212.
21. C. Cazorla, S. A. Shevlin and Z. X. Guo, *Phys. Rev. B*, 2010, **82**, 155454.
22. H. Lee, B. Huang, W. Duan and J. Ihm, *J. Appl. Phys*, 2010, **107**, 084304.
23. H. Lee, J. Ihm and M. L. Cohen, *Nano Lett*., 2010, **10**, 793.
24. I. Lopez-Corral, E. German, A. Juan, M. A. Volpe and G. P. Brizuela, *Int. J. Hydrog. Energy*, 2012, **37**, 6653.
25. Y. Liu, C. M. Brown, D. A. Neumann, D. B. Geohegan, A. A. Puretzky, C. M. Rouleau, H. Hu, D. Styers-Barnett, P. O. Krasnov and B. I. Yakobson, *Carbon*, 2012, **50**, 4953.
26. A. Reyhani, S. Z. Mortazavi, S. Mirershadi, A. Z. Moshfegh, P. Parvin and A. N. Golikand, *J. Phys. Chem. C*, 2011, **115**, 6994.
27. K. Iyakutti, Y. Kawazoe, M. Rajarajeswari and V. J. Surya, *Int. J. Hydrog. Energy*, 2009, **34**, 370.
28. R. Kodi Pandyan, S. Seenithurai and M. Mahendran, *Int. J. Hydrog. Energy*, 2010, **36**, 3007.
29. S. Seenithurai, R. Kodi Pandyan, S. Vinodh Kumar and M. Mahendran, *Int. J. Hydrog. Energy*, 2013, **38**, 7376.
30. J. D. Cawley, "Encyclopedia of Materials: Science and Technology", Elsevier, 2nd ed., 2001, 529.
31. B. W. Darvelt, "Material science for Dentistry", Wood Head Publishing, 10th ed., 2018, 249.
32. S. Samavedi, L. K. Poindexter, M. V. Dyke and A. S. Goldstein, "Regenerative medicine applications in organ transplantation", Academic Press, 2014, 81.
33. Z. M. Ao, Q. Jiang, R. Q. Zhang, T. T. Tan and S. Li, *J. Appl. Phys.*, 2009, **105**, 074307.
34. Z. M. Ao, J. Yang, S. Li and Q. Jiang, *Chem. Phys. Lett*., 2008, **461**, 276.
35. Z. M. Ao and F. M. Peeters, *Phys. Rev. B*, 2010, **81**, 205406.
36. J. Carrete, R. C. Longo, L. J. Gallego, A. Vega and L. C. Balbas, *Phys. Rev. B*, 2012, **85**, 125435.